Biodegradable Porous Polymers through Emulsion Templating

Yulia Lumelsky and Michael S. Silverstein*

Department of Materials Engineering, Technion - Israel Institute of Technology, Haifa 32000, Israel

Received November 3, 2008; Revised Manuscript Received December 8, 2008

ABSTRACT: Highly porous, emulsion-templated polymers, polyHIPE, that are synthesized within high internal phase emulsions (HIPE) combine a fully interconnected open-pore structure with mechanical integrity and the ability to absorb relatively large amounts of liquid through capillary action. Biodegradable polyHIPE would be of interest for tissue engineering scaffold applications. This paper describes the synthesis of both styrene-based and acrylate-based polyHIPE containing as much as 50 wt % of a biodegradable polycaprolactone (PCL) oligomer. The addition of PCL destabilizes the HIPE, yielding a partial collapse of the porous structure. This collapse yields a decrease in the relative mass of water absorbed, although the volumetric ratio of water absorbed to pore volume increases. The relatively low modulus, acrylate-based polyHIPE with 50% PCL underwent swelling, absorbing more than twice its pore volume. This polyHIPE also underwent extensive degradation, indicating that the PCL degradation promotes the disintegration of the macromolecular structure.

Introduction

PolyHIPE are highly porous, emulsion-templated, cross-linked polymers typically synthesized within a water-in-oil (W/O) high internal phase emulsion (HIPE) whose dispersed, aqueous phase occupies more than 74% of the volume.[1−3] During polymerization, holes develop within the thin envelope of continuous phase that surrounds the discrete droplets. The droplets become interconnected through these holes, yielding a bicontinuous phase structure. The porous morphology and properties of polyHIPE can be modified through variations in the HIPE contents and through variations in the synthesis conditions.[4−7] A variety of polyHIPE and polyHIPE-based materials have been synthesized including copolymers,[8−10] interpenetrating polymer networks (IPN),[11] crystallizable side chain polymers,[12−14] hydrogels (using O/W HIPE),[15−18] biocompatible polymers,[19−28] functional surfaces,[29,30] organic−inorganic hybrids,[31,32] and composites.[33−40]

PolyHIPE combine a fully interconnected, highly porous structure, a low bulk density, a high permeability, and a high surface area with mechanical integrity. In addition, polyHIPE can absorb relatively large amounts of liquid through capillary action. Thus polyHIPE, especially biodegradable polyHIPE, would be of interest for three-dimensional cell culture and tissue engineering scaffold applications.[19,20,23−26,41] The synthesis of polyHIPE containing biodegradable polymers is not straightforward since the presence of both an organic and an aqueous phase within HIPE limits the type of polymerization reactions that can be used. The methods that have been used successfully to incorporate biodegradable polymers within polyHIPE involve either copolymerization or semi-IPN formation with a biodegradable oligomer.[19−22] In previous work with styrene-based polyHIPE, it was shown that a copolymer containing 25 wt % of a biodegradable polycaprolactone (PCL) oligomer had a higher PCL content than a semi-IPN containing 40 wt % PCL oligomer. The unexpectedly low PCL content in the semi-IPN resulted from its removal during emulsifier extraction.[22]

This paper describes the synthesis of either styrene (S) based or 2-ethylhexyl acrylate (EHA) based polyHIPE that contain as much as 50 wt % PCL oligomer. Poly(2-ethylhexyl acrylate) (PEHA) is a biocompatible polymer that has been used in biomedical applications.[42] Polystyrene (PS), a glassy polymer with a high degree of chemical stability, is quite different from PEHA, a rubbery polymer with an ester group that can undergo hydrolytic attack. The differences between PS and PEHA are expected to be reflected in the polyHIPE's mechanical and thermal properties, in the polyHIPE's ability to absorb water, and in the polyHIPE's hydrolytic degradation.

* To whom correspondence should be addressed. E-mail: michaels@tx.technion.ac.il. Telephone: 972-4-829-4582. Fax: 972-4-829-5677.

Experimental Section

Materials. Styrene (Fluka Chemie), 2-ethylhexyl acrylate (Aldrich), and divinylbenzene (DVB, which contains 40% ethylstyrene, Riedel-de-Haen) were washed to remove the inhibitor (three times with an aqueous solution of 5 wt % sodium hydroxide (NaOH, Frutarom, Israel) and then three times with deionized water). An oligomeric PCL diol (PCL-OL, M_n = 530, Aldrich) was used as received to synthesize vinyl-terminated PCL (PCL-VL). For polyHIPE synthesis, the emulsifier was sorbitan monooleate (SMO, Span 80, Fluka Chemie), and the water-soluble initiator was potassium persulfate ($K_2S_2O_8$, Riedel-de-Haen). Potassium sulfate (K_2SO_4, Frutarom, Israel) was the water-soluble stabilizer used to enhance the rigidity of the interface since it is known to have a large salting-out effect and is thus a more effective stabilizer.[43,44]

PCL-VL Synthesis. Dichloromethane (DCM, Aldrich), triethylamine (TEA, Aldrich), anhydrous magnesium sulfate ($MgSO_4$, Aldrich), potassium hydrate (KOH, Riedel-de-Haen) and hydrochloric acid (HCl, Riedel-de-Haen) were used as received, while the acryloyl chloride (AC, Aldrich) was distilled before use. The synthesis of PCL-VL from PCL-OL by modification with AC has been described in detail elsewhere.[45] Briefly, a flask was charged with PCL-OL dissolved in DCM containing TEA. An addition funnel was charged with freshly distilled AC dissolved in DCM. The system was then purged with nitrogen gas and the flask cooled by immersion in an ice bath. The AC solution was added dropwise with stirring to the solution of the PCL-OL for about 1 h and the reaction was allowed to proceed for 8 h in the ice bath. The resulting solution was filtered to remove the triethylamine hydrochloride crystals produced during the reaction. The filtered solution was extracted with a 1% aqueous HCl solution and then with a 3% aqueous KOH solution until the aqueous layer remained colorless. The organic layer was dried over $MgSO_4$ and filtered. The excess solvent was removed by drying in a vacuum oven at 50 °C.

PolyHIPE Synthesis. The polyHIPE synthesis procedure has been described in detail elsewhere.[32] The composition, mass ratios and molar ratios for the various polyHIPE synthesized are listed in Table 1. The polyHIPE are labeled in a manner that indicates the monomer (S or EHA), the cross-linking comonomer (B for DVB and L for PCL-VL), and the mass percent of cross-linking comonomer. Thus, E-L50 indicates an EHA-based polyHIPE

10.1021/ma802461m CCC: $40.75
Published on Web 02/06/2009

Table 1. HIPE Compositions

sample	monomer	cross-linker	monomer/cross-linker wt %	monomer/cross-linker mol %
S-B10	S	DVB	90/10	91.8/8.2
S-L10	S	PCL-VL	90/10	98.2/1.8
S-L25	S	PCL-VL	75/25	94.8/5.2
S-L50	S	PCL-VL	50/50	86.0/14.0
E-B15	E	DVB	85/15	80.0/20.0
E-L50	E	PCL-VL	50/50	77.6/22.4

Table 2. PolyHIPE Properties

sample	ρ_f, g/cm^3	tan δ peaks, °C	E_f, Pa	E_p, Pa
S-B10	0.09	129.5	1.2×10^7	1.5×10^9
S-L10	0.12	−30.1, 88.0	2.8×10^6	2.0×10^8
S-L25	0.18	−18.1, 76.4	7.8×10^5	2.4×10^7
S-L50	0.34	−5.9, 65.8	7.6×10^5	6.6×10^6
E-B15	0.12	−17.9	1.3×10^5	9.0×10^6
E-L50	0.51	−35.5	7.0×10^4	2.7×10^5

Table 3. Water Absorption and PolyHIPE Degradation

sample	plateau values r_m, wt %	plateau values r_v, vol %	m_R, wt %
S-B10	944	89.8	100.0
S-L10	973	90.5	88.2
S-L25	430	93.4	65.6
S-L50	204	98.6	39.7
E-B15	729	94.7	100.0
E-L50	277	221	0.0

containing 50 wt % PCL-VL in the feed. The stability of the HIPE containing PCL-VL was enhanced by raising the emulsifier content from 20% of the monomer's mass, used for the HIPE that did not contain PCL, to 40% of the monomer's mass.

The mass ratio of the organic phase to the aqueous phase was maintained at around 12/88 for all the syntheses. Briefly, the aqueous phase was added slowly to the organic phase (S or EHA, DVB or PCL-VL, and SMO) with continuous stirring. Polymerization took place in a convection oven at 65 °C for 24 h. The polyHIPE was dried in a vacuum oven at room temperature for about 48 h until a constant weight was achieved and then washed in deionized water at 80 °C under constant stirring for 24 h. The polyHIPE was then dried in a vacuum oven at room temperature for 24 h.

Characterization. The molecular structure was characterized using Fourier transform infrared spectroscopy (FTIR, from 400 to 4000 cm^{-1} at a resolution of 2 cm^{-1}, Equinox 55 FTIR, Brucker) using a photoacoustic attachment (MTEC Model 300). The density of the polyHIPE, ρ_f, was determined using gravimetric analysis. The measurement of at least seven samples yielded a typical error of 0.004 g/cm^3. The porous structure was characterized using high resolution scanning electron microscopy (HRSEM, Zeiss LEO 982) with uncoated specimens and an accelerating voltage of 1−3 kV. Several micrographs were analyzed for each sample to generate a statistical depiction of the average. A statistical correction was used to account for the arbitrary, nonequatorial, location of the section.[4]

Differential scanning calorimetry (DSC) was carried out by heating from −100 to +200 °C at a rate of 10 °C/min in nitrogen (Mettler DSC-821). Dynamic mechanical thermal analysis (DMTA) temperature sweeps from −100 to +200 °C were conducted at a rate of 3 °C/min and a frequency of 1 Hz in compression (MK III DMTA, Rheometrics) on 10 × 10 × 10 mm^3 specimens. Uniaxial compressive stress−strain measurements were conducted at 25 °C on 5 × 5 × 5 mm^3 specimens until an equipment-related force limitation was reached (MK III DMTA, Rheometrics). The modulus, E_f, was calculated from the slope of the stress−strain curve at low strains.

The mass of water imbibed per mass polyHIPE, m_w, was studied as a function of time. PolyHIPE specimens 5 × 5 × 5 mm^3 were placed in a water-filled vial and held underneath the surface using a weight. The specimens were removed from the vial, blotted, weighed, and replaced. The water absorption mass ratio, r_m, is the ratio between the mass of water imbibed, m_w, and the mass of the original polyHIPE specimen, m_f. The volumetric water absorption ratio, r_v, is the ratio between the volume of water imbibed and the volume of the pores in the original polyHIPE and was calculated using eq 1

$$r_v = \left(\frac{m_w}{\rho_w}\right)\left(\frac{\rho_p \rho_f}{m_f(\rho_p - \rho_f)}\right) \quad (1)$$

where ρ_w is the density of water (1 g/cm^3) and ρ_p is the density of the polymer (assumed to be 1 g/cm^3 in this work).

The hydrolytic degradation of the polyHIPE was studied as a function of time. NaOH was used to accelerate the hydrolysis. PolyHIPE specimens 9 × 7 × 1 mm^3 were placed in vials containing 10 mL of a 3 M aqueous solution of NaOH at room temperature and the solution was changed weekly. The samples were removed, rinsed with deionized water, and then dried in a vacuum oven at room temperature for 24 h (a constant weight was achieved) at designated time intervals. The residual mass, m_R, is the mass of the hydrolyzed specimen divided by the mass of the original specimen.

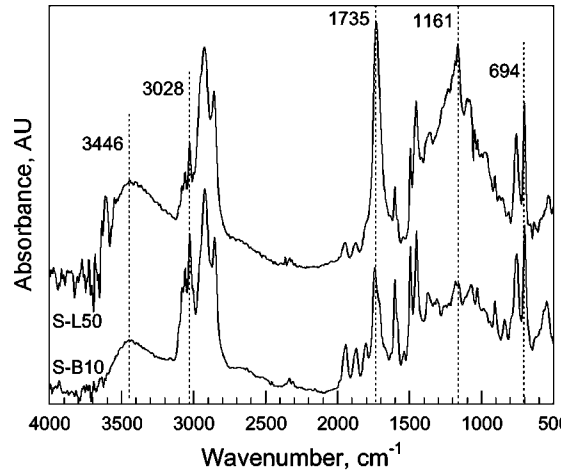

Figure 1. FTIR spectra from S-B10 and S-L50.

Results and Discussion

Molecular Structure. The terminal hydroxyl groups of PCL-OL were successfully substituted with vinyl groups yielding PCL-VL, as shown through the changes in the FTIR spectra (not shown).[22] FTIR was also used to confirm the incorporation of PCL into the S- and EHA-based polyHIPE copolymers. The FTIR spectra of S-B10 and S-L50 are seen in Figure 1. The absence of a C═C band at 1636−1620 cm^{-1}, indicates that all the vinyl groups have reacted. The S-based polyHIPE exhibit bands at 3028 and 694 cm^{-1} associated with the aromatic C−H stretching and C−H out-of-plane bending, respectively.[46] The PCL-containing polyHIPE exhibit C═O bands at 1735 cm^{-1} and C−O bands at 1161 cm^{-1}.[46] The effects of feed composition on the intensities of the C═O and C−O bands were studied by normalizing their intensities by the intensity of the band at 694 cm^{-1} that is associated with styrene. The normalized intensities of the C═O and C−O bands increase in a linear fashion with increasing PCL content, as seen in Figure 2. The broad C−OH stretching band at 3446 cm^{-1} in both S-B10 and S-L50 is associated with residual surfactant.

PolyHIPE Structure. The densities of S-B10 and E-B15, the DVB cross-linked polyHIPE, are 0.09 and 0.12 g/cm^3, respectively (Table 2). Densities of around 0.1 g/cm^3 can be expected from ratio of the organic phase volume to the aqueous phase volume. The densities of the polyHIPE cross-linked using PCL-VL are higher than those cross-linked using DVB (Table

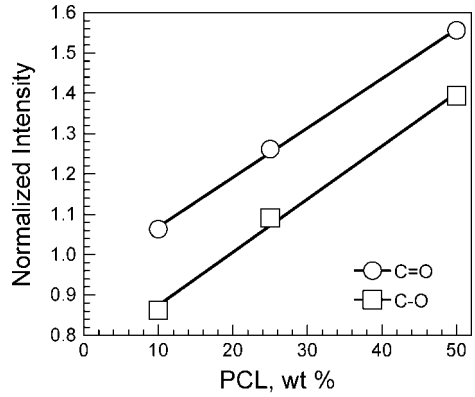

Figure 2. Variation of the normalized intensities of the carbonyl band at 1735 cm^{-1} and the ether band at 1161 cm^{-1} with PCL content for the S-based polyHIPE. The intensities were normalized by the intensity of the aromatic CH band at 694 cm^{-1}.

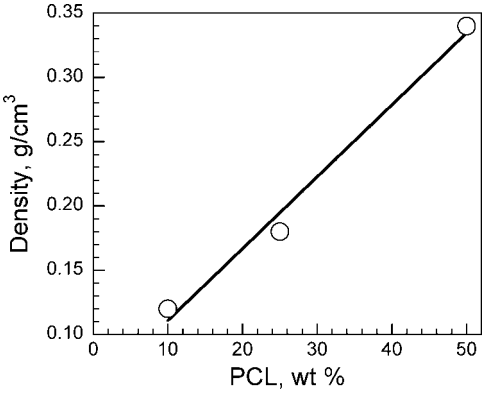

Figure 3. Variation of polyHIPE density with PCL content for the S-based polyHIPE.

2). The density of the S-based polyHIPE increases in a linear fashion with the PCL content (Figure 3). The PCL oligomer is relatively flexible compared to DVB. The increased flexibility of the molecular network reduces the resistance to the capillary forces generated during drying, thus enhancing the tendency to collapse. The partial collapse of these more flexible polyHIPE yields the increase in density, which reaches 0.34 g/cm^3 for S-L50. While PS has a glass transition temperature, T_g, that is above room temperature (105 °C), PEHA has a T_g that is significantly below room temperature (−40 °C).[47] The EHA-based polyHIPE are, therefore, more flexible than the S-based polyHIPE, resulting in a more extensive collapse during drying and yielding an even higher density, reaching 0.51 g/cm^3 for E-L50.

The porous structures of the polyHIPE are seen in Figure 4 and Figure 5. S-B10 exhibits a typical polyHIPE structure (Figure 4a,b). The void diameters range from 20 to 35 μm, reflecting the size of the water droplets in the HIPE, and the hole diameters range from 1 to 6 μm. S-L10 has a polyHIPE-like, highly porous interconnected structure with a significantly larger void size and a significantly broader void size distribution than that of S-B10 (Figure 4c−e). The voids range from 35 to 95 μm and the walls contain a high density of holes 4 to 16 μm in diameter. The porous structure of S-L50 is significantly different (Figure 4f−h). S-L50 consists of partially collapsed, interconnected voids ranging from 25 to 45 μm and separated by relatively thick, porous, walls (Figure 4g). The addition of significant amounts of PCL into the HIPE increases the viscosity and decreases the hydrophobicity of the external organic phase leading to HIPE destabilization and droplet coalescence.[33]

The addition of PCL-VL to EHA-based polyHIPE had an even more significant destabilizing effect. E-B15 has voids of around 12 μm in diameter, a narrow void size distribution, and holes of around 2 μm in diameter (Figure 5a,b). E-L50, on the other hand, exhibits a distorted structure (Figure 5c−e), reflecting the collapse during drying that yields its relatively high density. The voids of E-L50 range from 230 to 580 μm (not shown) and the walls have a nodular porous structure (Figure 5e). Here again, the addition of PCL reduces HIPE stability and results in droplet coalescence.

Thermal and Mechanical Properties. The low molecular weight PCL does not crystallize within the polyHIPE, as seen through DSC characterization (not shown). DMTA temperature sweeps of the S-based polyHIPE are presented in Figure 6 and the tan δ peak temperatures are listed in Table 2. S-B10 has one tan δ peak at 130 °C, reflecting the high degree of cross-linking and the low thermal conductivity of the polyHIPE.[11,31] Interestingly, all the S-based, PCL-containing polyHIPE have two tan δ peaks and the positions of the peaks depend on the PCL content. The lower tan δ peak, T_{g1}, represents a PCL-rich phase while the higher tan δ peak, T_{g2}, represents a S-rich phase. The variations of the tan δ peak temperatures as function of the PCL content for the S-based polyHIPE are seen in Figure 7. T_{g1} increases by approximately 24 °C with increasing PCL content, while T_{g2} decreases by approximately 22 °C. The height of T_{g1}, which is associated with PCL, increases with increasing PCL content. The increase in the temperature of T_{g1} reflects the increase in cross-link density which limits the segmental mobility of the macromolecular network. T_{g2}, which is associated with PS, moves to lower temperature and its height decreases with increasing PCL content. These changes in T_{g2} reflect the decrease in the styrene content and the resulting increase in segmental mobility. The glass transition temperatures of PEHA and PCL are −40 and −62 °C, respectively.[47,48] The DMTA temperature sweep of E-L50 exhibits one peak at −36 °C, below the tan δ peak at −18 °C observed for E-B15 (Table 2).

Room-temperature compressive stress−strain curves for selected S-based polyHIPE are seen in Figure 8. The stress−strain curves are typical of polyHIPE, exhibiting a linear elastic region at low strains, a stress plateau region, and a densification region with a rapid rise in stress. The EHA-based polyHIPE recovered their original shapes when the stress was removed.

S-B10 was relatively stiff, reflecting its tan δ peak of 130 °C, with a modulus of 1.2×10^7 Pa. E-B15 was relatively elastomeric, reflecting its tan δ peak of −18 °C, with a modulus of 1.3×10^5 Pa, 2 orders of magnitude smaller than that of S-B10. The moduli of the PCL-cross-linked polyHIPE were significantly lower than the moduli of the DVB-cross-linked polyHIPE (Table 2), reflecting the relative flexibility of the PCL oligomer compared to the relatively rigidity of DVB.

The relative modulus of open cell foams (E_f divided by the modulus of the polymer that makes up the wall, E_p) has been related to the square of the relative density (ρ_f divided by ρ_p), as seen in eq 2.[49]

$$\frac{E_f}{E_p} = \left(\frac{\rho_f}{\rho_p}\right)^2 \tag{2}$$

For a given polymer, a 5-fold increase in density is, therefore, expected to produce a 25-fold increase modulus. In these polyHIPE, however, the increase in density with increasing PCL content produced, instead, a drastic reduction in modulus (Table 2). This reduction in modulus, however, is associated with the reduction in the modulus of the polymer comprising the polyHIPE, reflecting the changes in macromolecular structure. The modulus of the polymer was calculated from the measured E_f and the measured ρ_f, assuming a ρ_p of 1 g/cm^3 (Table 2).

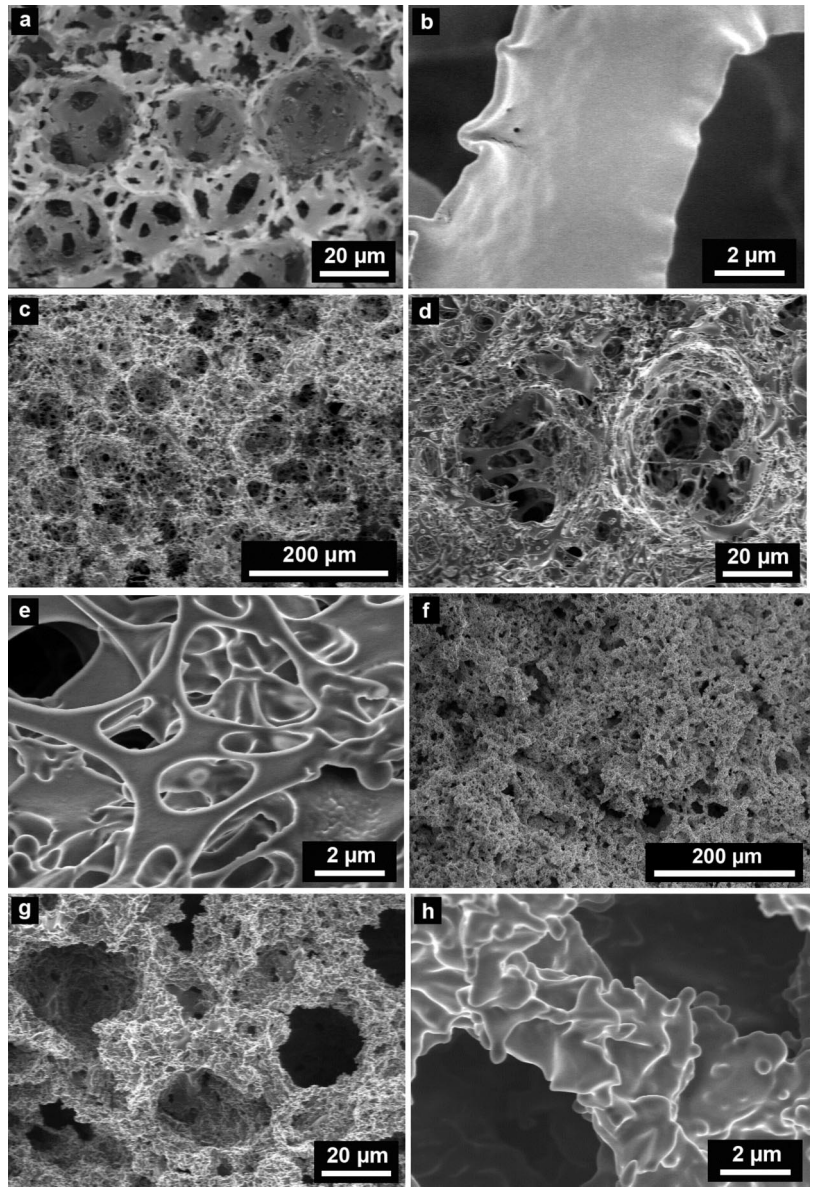

Figure 4. HRSEM micrographs of S-based polyHIPE fracture surfaces: (a, b) S-B10; (c, d, e) S-L10; (f, g, h) S-L50.

The E_p of 1.5×10^9 Pa for S-B10 reflects its glassy nature and the E_p of 9.0×10^6 Pa for E-B15 reflects its elastomeric nature. Incorporating the flexible PCL oligomer into the molecular structure produces orders of magnitude reductions in E_p, both for the S-based and for the EHA-based polyHIPE (Table 2). These reductions in E_p reflect the increase in segmental mobility that is indicated by the reduction in the higher tan δ peak temperature for the S-based polyHIPE.

Water Absorption. The variation of r_m, the relative mass of water absorbed, with time for the S-based polyHIPE is seen in Figure 9. The r_m plateau values for the S-based and EHA-based polyHIPE are listed in Table 3. S-B10 and E-B15 absorb relatively large amounts of water (plateau values of 944 and 730 wt %, respectively) owing to the presence of residual surfactant. S-B10 that has undergone extraction in methanol to remove the surfactant does not readily imbibe water.[1,50] The polyHIPE containing PCL absorb less water, reflecting their higher densities. However, r_v, the relative volume of water absorbed, increases with PCL content, as seen in Table 3. The variations of the r_m and r_v plateau values with PCL content for the S-based polyHIPE are seen in Figure 10. Around 90 vol % of the pores are filled with water, even at low PC contents. For S-L50, over 98 vol % of the pores are filled with water.

Interestingly, E-L50 exhibits a r_v plateau of 221 vol %. This indicates that the volume of water absorbed is more than double the volume of the empty pores in the original polyHIPE. E-L50 swells when immersed in water, expanding the pores and increasing the pore volume. The swelling in E-L50, with its extremely low modulus, results from the deformations induced by the stresses generated during water uptake through capillary action.

Degradation. PCL is a hydrolytically degradable polyester. Hydrolytic degradation occurs by random cleavage of the ester links in the polymer network followed by dissolution of the fragments. S-B10, E-B15, S-L50, and E-L50 were immersed in a 3 M aqueous solution of NaOH for 10 weeks. The variation of residual mass with time is seen in Figure 11. S-B10 and E-B15 do not contain PCL and neither exhibited mass loss during the entire 10 week period. In contrast, both S-L50 and E-L50 exhibited similar mass losses of around 50% during the first week. This extensive mass loss during the first week reflects the degradation of the polymer network through hydrolytic

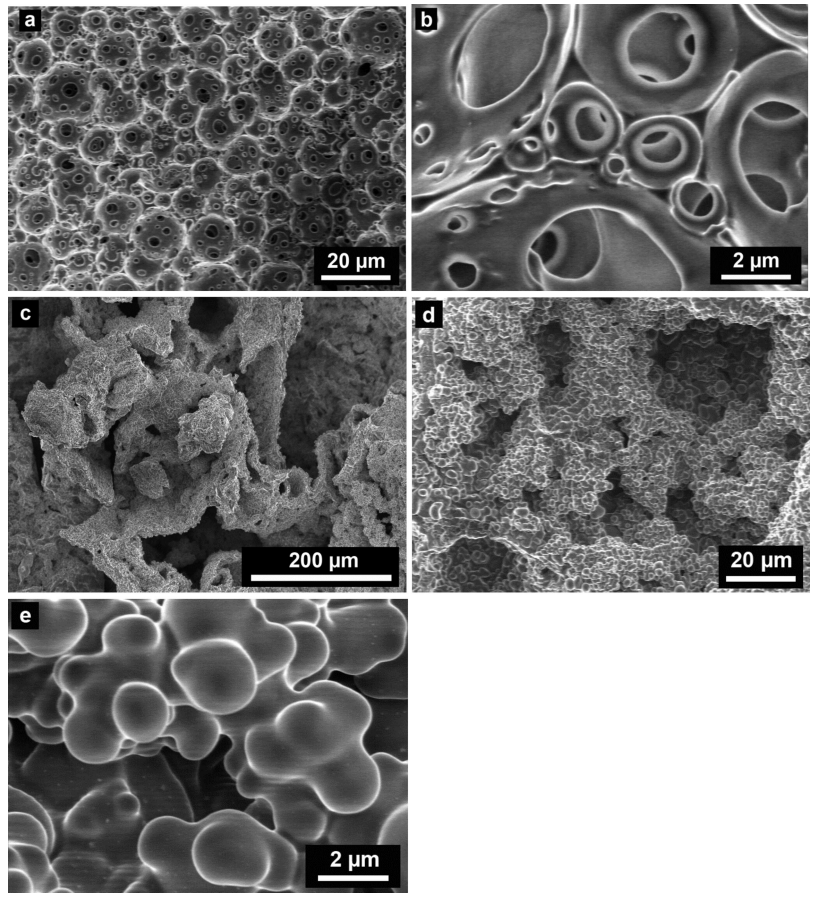

Figure 5. HRSEM micrographs of EHA-based polyHIPE fracture surfaces: (a, b) E-B15; (c, d, e) E-L50.

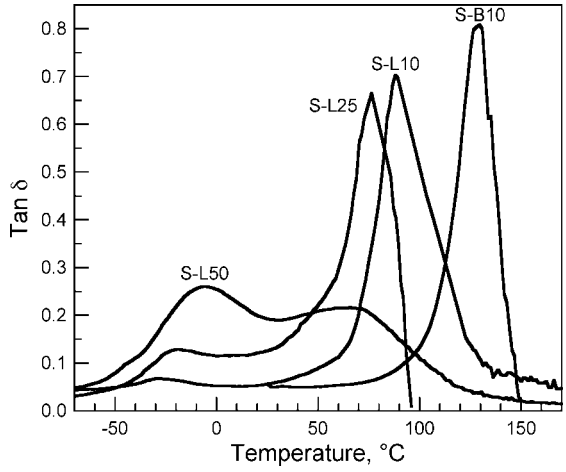

Figure 6. Variation of tan δ with temperature for the S-based polyHIPE.

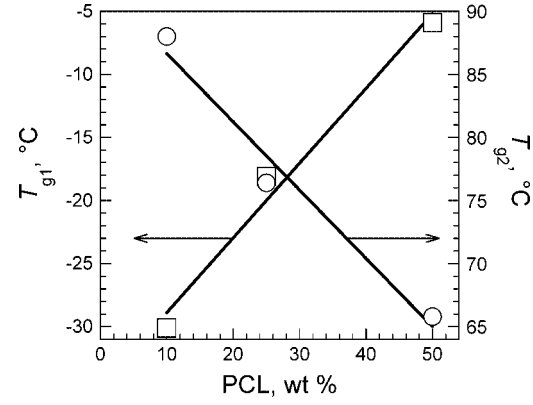

Figure 7. Variation of (□) T_{g1} and (○) T_{g2} with PCL content for the S-based polyHIPE.

degradation of the PCL. In the following weeks S-L50 exhibited an additional mass loss of around 10%, while E-L50 underwent complete degradation.

The FTIR spectrum from the residual S-L50 following 10 weeks in the NaOH solution is somewhat similar to that from the as-synthesized S-L50 (Figure 12). There are, however, some changes in the relative intensities of the OH (3446 cm^{-1}), CH_2 (2853 cm^{-1}), C═O (1735 cm^{-1}), and O−C (1161 cm^{-1}) bands. In addition, the degraded S-L50 exhibits a prominent band at 1565 cm^{-1} associated with COOH that does not appear in the as-synthesized S-L50. The effects of degradation on these band heights, normalized by the height of the aromatic CH band at 694 cm^{-1}, are seen in Figure 13. The reduction in the normalized intensities of the CH_2, C═O, and C−O bands indicates that the PCL content was reduced through degradation. The degradation of the PCL produces COOH groups, hence the appearance of a prominent band at 1565 cm^{-1} in the degraded S-L50. Interestingly, the change in the normalized intensity of the OH band is relatively small. While the OH band in the as-synthesized S-L50 reflects the presence of residual surfactant, the OH band in the hydrolyzed S-L50 reflects the presence of COOH groups.

While the residual mass of S-L50 is 40% following 10 weeks in the NaOH solution, E-L50 has undergone complete degradation. The differences in degradation between the S-based and EHA-based polyHIPE reflect the differences between PS and PEHA. While PS is a glassy polymer with a relatively high chemical resistance, PEHA is rubbery polymer containing ester

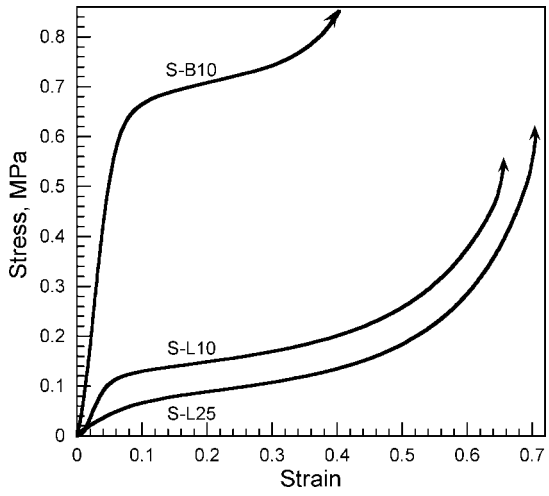

Figure 8. Compressive stress−strain curves for S-B10, S-L10, and S-L25.

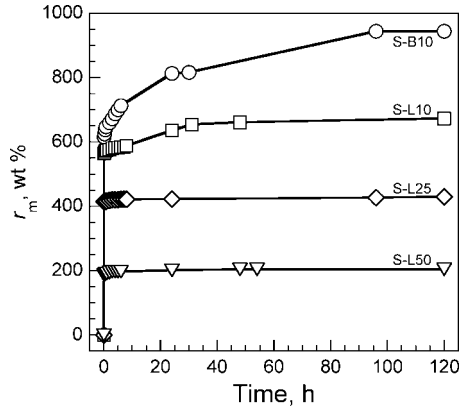

Figure 9. Variation of r_m with time for the S-based polyHIPE.

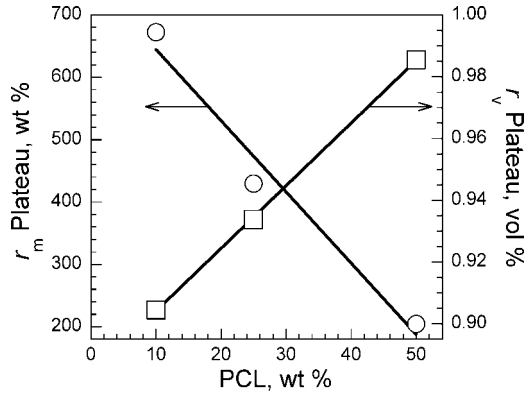

Figure 10. Variation of the (○) r_m and (□) r_v plateaus with PCL content for the S-based polyHIPE.

groups that could undergo hydrolysis. However, it is interesting to note that E-B15 (EHA cross-linked with DVB) did not undergo any degradation under the same conditions that E-L50 (EHA cross-linked with 50 wt % PCL) underwent complete degradation. It seems that the degradation of PCL causes the entire macromolecular structure to disintegrate. The mechanisms through which the degradation of PCL causes this disintegration and the molecular masses of the fragments produced are currently under investigation. Preliminary cell growth results, to be presented in a future manuscript, indicate that cell growth and cell penetration into the polyHIPE are far superior in the EHA-based polyHIPE compared to the styrene-based polyHIPE controls.

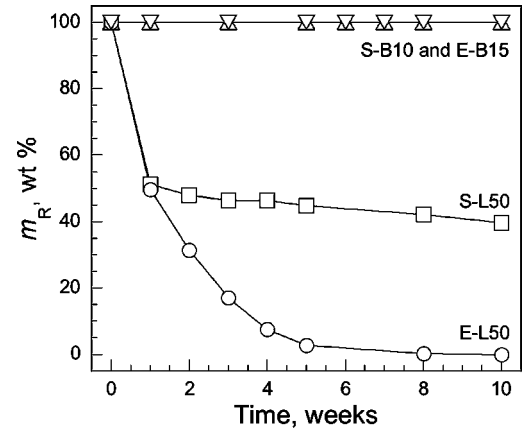

Figure 11. Variation of m_R with time for S-B10, S-L50, E-B15, and E-L50 immersed in a 3 M aqueous solution of NaOH.

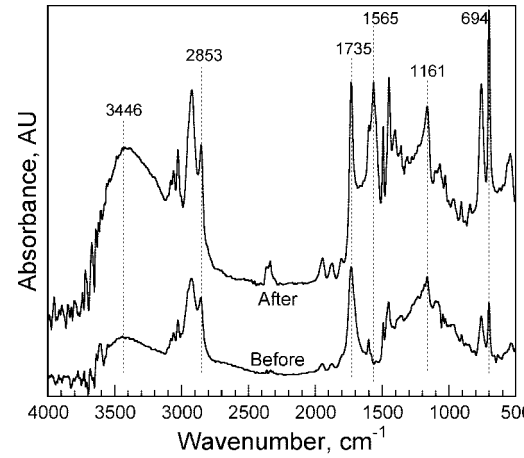

Figure 12. FTIR spectra from S-L50 before and after degradation.

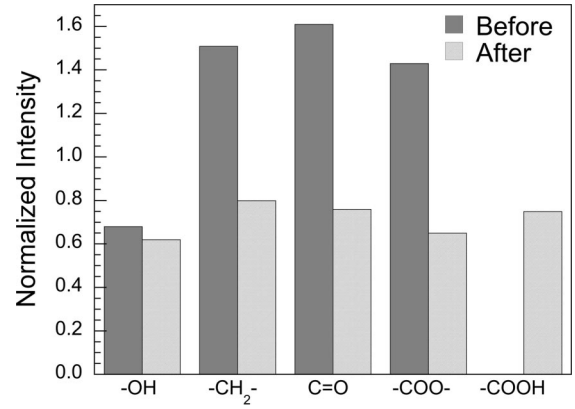

Figure 13. Normalized FTIR band intensities from S-L50 before and after degradation. The intensities were normalized by the intensity of the aromatic CH band at 694 cm^{-1}.

Conclusions

Porous styrene-based and EHA-based polyHIPE cross-linked with a vinyl terminated PCL have been synthesized using emulsion templating. The addition of PCL destabilized the HIPE, more significantly for acrylate-based HIPE than for S-based HIPE, yielding partial collapse during polymerization and a density of 0.51 g/cm^3 for an EHA-based polyHIPE with 50% PCL. The mass ratio of water absorbed to polyHIPE decreased with increasing PCL content, resulting from the increase in polyHIPE density. However, the volumetric ratio of water absorbed to pore volume increased with PCL content. Most

significantly for cell-growth applications, the relatively low modulus, EHA-based polyHIPE with 50% PCL, unlike the styrene-based polyHIPE, underwent swelling, absorbing more than twice its pore volume, and also underwent complete degradation. The complete degradation of the EHA-based polyHIPE indicates that the degradation of PCL promotes the disintegration of the macromolecular structure.

References and Notes

(1) Cameron, N. R.; Sherrington, D. C. *Adv. Polym. Sci.* **1996**, *126*, 163.
(2) Cameron, N. R. *Polymer* **2005**, *46*, 1439.
(3) Cameron, N. R.; Sherrington, D. C.; Albiston, L.; Gregory, D. P. *Colloid Polym. Sci.* **1996**, *274*, 592.
(4) Carnachan, R. J.; Bokhari, M.; Przyborski, S. A.; Cameron, N. R. *Soft Matter* **2006**, *2*, 608.
(5) Barbetta, A.; Dentini, M.; Zannoni, E. M.; DeStefano, M. E. *Langmuir* **2005**, *21*, 12333.
(6) Barbetta, A.; Cameron, N. R. *Macromolecules* **2004**, *37*, 3202.
(7) Barbetta, A.; Cameron, N. R. *Macromolecules* **2004**, *37*, 3188.
(8) Sergienko, A.; Tai, H.; Narkis, M.; Silverstein, M. S. *J. Appl. Polym. Sci.* **2004**, *94*, 2233.
(9) Leber, N.; Fay, J. D. B.; Cameron, N. R.; Krajnc, P. *J. Polym. Sci., Part A: Polym. Chem.* **2007**, *45*, 4043.
(10) Sergienko, A.; Tai, H.; Narkis, M.; Silverstein, M. S. *J. Appl. Polym. Sci.* **2002**, *84*, 2018.
(11) Tai, H.; Sergienko, A.; Silverstein, M. S. *Polym. Eng. Sci.* **2001**, *41*, 1540.
(12) Livshin, S.; Silverstein, M. S. *Macromolecules* **2007**, *40*, 6349.
(13) Livshin, S.; Silverstein, M. S. *Macromolecules* **2008**, *41*, 3930.
(14) Livshin, S.; Silverstein, M. S. *Soft Matter* **2008**, *4*, 1630.
(15) Kulygin, O.; Silverstein, M. S. *Soft Matter* **2007**, *2*, 1525.
(16) Butler, R.; Davies, C. M.; Cooper, A. I. *Adv. Mater.* **2001**, *13*, 1459.
(17) Butler, R.; Hopkinson, I.; Cooper, A. I. *J. Am. Chem. Soc.* **2003**, *125*, 14473.
(18) Gitli, T.; Silverstein, M. S. *Soft Matter* **2008**, *4*, 2475.
(19) Busby, W.; Cameron, N. R.; Jahoda, C. A. B. *Biomacromolecules* **2001**, *2*, 154.
(20) Busby, W.; Cameron, N. R.; Jahoda, C. A. B. *Polym. Int.* **2002**, *51*, 871.
(21) Christenson, E. M.; Soofi, W.; Holm, J. L.; Cameron, N. R.; Mikos, A. G. *Biomacromolecules* **2007**, *8*, 3806–3814.
(22) Lumelsky, J.; Zoldan, J.; Levenberg, S.; Silverstein, M. S. *Macromolecules* **2008**, *41*, 1469.
(23) Hayman, M. W.; Smith, K. H.; Cameron, N. R.; Przyborski, S. A. *Biochem. Biophys. Methods* **2005**, *62*, 231.
(24) Hayman, M. W.; Smith, K. H.; Cameron, N. R.; Przyborski, S. A. *Biochem. Biophys. Res. Commun.* **2004**, *314*, 483.
(25) Bokhari, M. A.; Akay, G.; Zhang, S. G.; Birch, M. A. *Biomaterials* **2005**, *26*, 5198.
(26) Akay, G.; Birch, M. A.; Bokhari, M. A. *Biomaterials* **2004**, *25*, 3991.
(27) Krajnc, P.; Stefanec, D.; Pulko, I. *Macromol. Rapid Commun.* **2005**, *26*, 1289.
(28) Stefanec, D.; Krajnc, P. *React. Funct. Polym.* **2005**, *65*, 37.
(29) Mercier, A.; Deleuze, H.; Maillard, B.; Mondain-Monval, O. *Adv. Synth. Catal.* **2002**, *344*, 33.
(30) Moine, L.; Deleuze, H.; Maillard, B. *Tetrahedron Lett.* **2003**, *44*, 7813.
(31) Tai, H.; Sergienko, A.; Silverstein, M. S. *Polymer* **2001**, *42*, 4473.
(32) Silverstein, M. S.; Tai, H.; Sergienko, A.; Lumelsky, Y.; Pavlovsky, S. *Polymer* **2005**, *46*, 6682.
(33) Normatov, J.; Silverstein, M. S. *Polymer* **2007**, *48*, 6648.
(34) Normatov, J.; Silverstein, M. S. *Macromolecules* **2007**, *40*, 8329.
(35) Normatov, J.; Silverstein, M. S. *Chem. Mater.* **2008**, *20*, 1571.
(36) Normatov, J.; Silverstein, M. S. *J. Polym. Sci. A: Polym. Chem.* **2008**, *46*, 2357.
(37) Menner, A.; Powell, R.; Bismarck, A. *Soft Matter* **2006**, *4*, 337.
(38) Haibach, K.; Menner, A.; Powell, R.; Bismarck, A. *Polymer* **2006**, *47*, 4513.
(39) Menner, A.; Haibach, K.; Powell, R.; Bismarck, A. *Polymer* **2006**, *47*, 7628.
(40) Desforges, A.; Backov, R.; Deleuze, H.; Mondain-Monval, O. *Adv. Funct. Mater.* **2005**, *15*, 1689.
(41) Ciardelli, G.; Chiono, V.; Cristallini, C.; Barbani, N.; Ahluwalia, A.; Vozzi, G.; Previti, A.; Tantussi, G.; Giusti, P. *J. Mater. Sci.: Mater. Med.* **2004**, *15*, 305.
(42) Dumitriu, S. *Polymeric biomaterials*, 2nd ed.; Marcel Dekker: New York, 2002.
(43) Pons, R.; Solans, C.; Stebe, M. J.; Erra, P.; Ravey, J. C. *Prog. Colloid Polym. Sci.* **1992**, *89*, 110.
(44) Kunieda, H.; Yano, N.; Solans, C. *Colloids Surf.* **1989**, *36*, 313.
(45) Storey, R. F.; Warren, S. C.; Allison, C. J.; Wiggins, J. S. *Polymer* **1993**, *34*, 4365.
(46) Colthup, N. B.; Daly, L. H. *Introduction to infrared and Raman spectroscopy*, 3rd ed.; Academic Press: New York, 1990.
(47) Lee, W. A.; Knight, G. J. In *Polymer handbook*, 4th ed.; Brandrup, J., Immergut, E. H., Grulke, E. A., Eds.; John Wiley and Sons: New York, 1966.
(48) Orwoll, R. A. In *Physical properties of polymers handbook*; Mark, J. E., Ed.; American Institute of Physics: New York, 1996; p 81.
(49) Gibson, L. J.; Ashby, M. F. *Cellular Solids*, 2nd ed.; Cambridge University Press: Cambridge, U.K., 1997.
(50) Kulygin, O. *Porous hydrophilic polymers synthesized within high internal phase emulsions. Research Thesis,* Technion: Haifa, Israel, 2007.

MA802461M